$\mathrm{M}^{\mathrm{odeling}}\mathrm{M}\mathrm{C}^{\mathrm{omputing}}_{\mathrm{athematical}}$

Calculation of transverse piezoelectric characteristics of quasi-one-dimensional glycine phosphite ferroelectric

Vdovych A.[1], Zachek I.[2], Levitskii R.[1]

[1]*Institute for Condensed Matter Physics of the National Academy of Sciences of Ukraine,*
1 Svientsitskii Str., Lviv, 79011, Ukraine
[2]*Lviv Polytechnic National University, 12 S. Bandera Str., Lviv, 79013, Ukraine*

The model of the glycine phosphite crystal, modified by taking into account of piezoelectric coupling of ordering structure elements with the lattice strains, is used for investigation of piezoelectric characteristics of the crystal. In the frames of two-particle cluster approximation the transverse piezoelectric coefficients are calculated. The influences of hydrostatic, uniaxial pressures, shear stresses and transverse electric fields on the transverse piezoelectric coefficients of the crystal are studied.

Keywords: *ferroelectrics, phase transition, piezoelectric coefficients, pressure effects, external field effects.*

1. Introduction

Investigations of the effects appearing under mechanical stress or external electric field is one of actual problems of physics of ferroelectric materials, especially for glycine phosphite crystal (GPI), that belongs to the ferroelectric compounds with hydrogen bonds [1].

On the basis of the proton model [2], in [3] there was created the model of deformed GPI crystal, which takes into account the piezoelectric coupling between proton and lattice subsystems. In [3] the components of polarization vector, dielectric permittivity tensor, longitudinal piezoelectric coefficients, elastic constants and molar heat capacity were calculated; a satisfactory description of the experimental data is obtained. The model of deformed GPI crystal made it possible to describe correctly the influence of transverse fields $E_x\ E_z$ [6], hydrostatic pressure [4] and uniaxial pressures [5] on these characteristics.

However, the symmetry of strains ε_4, ε_6 was not taken into account correctly in [3] and the transverse piezoelectric coefficients e_{1j}, e_{3j}, h_{1j} and h_{3j} were not calculated. In [7] the GPI model [3] is modified for the case of decreasing of symmetry under shear stresses σ_{yz} and σ_{xy}. It was ascertained that the components of polarization vector P_x and P_z appear under the shear stresses σ_{yz} and σ_{xy}, and the transverse permittivities ε_{xx} and ε_{zz} diverge at T_c point.

In the present paper using the developed in [7] model of deformed GPI crystal the effects of hydrostatic and uniaxial pressures, shear stresses and transverse electric fields on the transverse piezoelectric characteristics of this crystal are studied.

2. Hamiltonian of the model

The model [7] consider the system of protons in GPI, localised on O-H...O bonds between phosphite groups HPO_3, which form zigzag chains along crystallographic c-axis of the crystal (see Fig. 1). For better understanding of the model only phosphite groups are shown in the figure. Dipole moments $\boldsymbol{d}_{qf}(f = 1,\dots,4)$ are ascribed to the protons on the bonds. In the ferroelectric phase the dipole
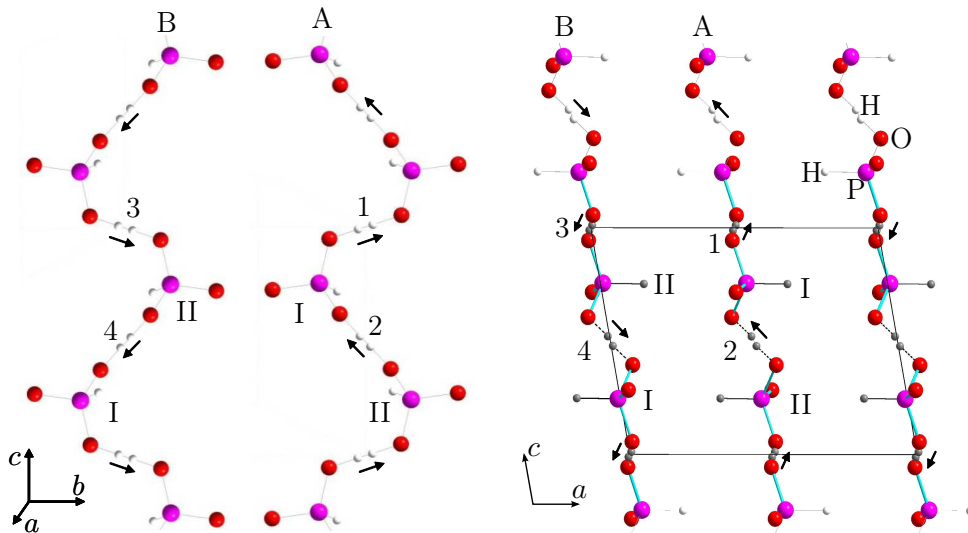
Fig. 1. Orientations of vectors $\boldsymbol{d}_{qf}$ in the primitive cell in the ferroelectric phase [3,7].

moments compensate each other ($\boldsymbol{d}_{q1}$ with $\boldsymbol{d}_{q3}$, $\boldsymbol{d}_{q2}$ with $\boldsymbol{d}_{q4}$) in directions Z and X (X $\perp$ (b,c), Y $\parallel$ b, Z $\parallel$ c), and simultaneously supplement each other in direction Y, creating spontaneous polarization.

Pseudospin variables $\frac{\sigma_{q1}}{2}, \ldots, \frac{\sigma_{q4}}{2}$ describe reorientation of the dipole moments of the base units: $\boldsymbol{d}_{qf} = \boldsymbol{\mu}_f \frac{\sigma_{qf}}{2}$. Mean values $\langle \frac{\sigma}{2} \rangle = \frac{1}{2}(n_a - n_b)$ are connected with differences in occupancy of the two possible molecular positions, n_a and n_b.

Below for the components of the vectors and tensors we use the notations 1, 2 and 3 instead of x, y and z for convenience. Hamiltonian of proton subsystem of GPI, which takes into account the short-range and long-range interactions and the applied electric fields E_1, E_2, E_3 along positive directions of the Cartesian axes X, Y and Z can be written in such a way [7]:

$$\hat{H} = NU_{\text{seed}} + \hat{H}_{\text{short}} + \hat{H}_{\text{long}} + \hat{H}_E, \tag{1}$$

where N is the total number of primitive cells. The term U_{seed} in (1) is the "seed" energy, which relates to the heavy ion sublattice and do not depends explicitly on configuration of the proton subsystem. It includes the elastic, piezoelectric and dielectric parts, expressed in terms of electric fields E_i ($i = 1, 2, 3$) and strains ε_j ($j = 1, \ldots, 6$).

$$U_{\text{seed}} = v \left(\frac{1}{2} \sum_{j,j'=1}^{6} c_{jj'}^{E0}(T)\varepsilon_j\varepsilon_{j'} - \sum_{i=1}^{3}\sum_{j=1}^{6} e_{ij}^0\varepsilon_j E_i - \sum_{i,i'=1}^{3} \frac{1}{2}\chi_{ii'}^{\varepsilon 0}E_i E_{i'} \right).$$

Parameters $c_{jj'}^{E0}(T)$, e_{ij}^0, $\chi_{ii'}^{\varepsilon 0}$ are so called "seed" elastic constants, "seed" coefficients of piezoelectric stresses and "seed" dielectric susceptibilities, respectively; v is volume of a primitive cell. Matrices $c_{jj'}^{E0}$, e_{ij}^0, $\chi_{ii'}^{\varepsilon 0}$ are given by:

$$\hat{c}_{jj'}^{E0} = \begin{pmatrix} c_{11}^{E0} & c_{12}^{E0} & c_{13}^{E0} & 0 & c_{15}^{E0} & 0 \\ c_{12}^{E0} & c_{22}^{E0} & c_{23}^{E0} & 0 & c_{25}^{E0} & 0 \\ c_{13}^{E0} & c_{23}^{E0} & c_{12}^{E0} & 0 & c_{35}^{E0} & 0 \\ 0 & 0 & 0 & c_{44}^{E0} & 0 & c_{46}^{E0} \\ c_{15}^{E0} & c_{25}^{E0} & c_{35}^{E0} & 0 & c_{55}^{E0} & 0 \\ 0 & 0 & 0 & c_{46}^{E0} & 0 & c_{66}^{E0} \end{pmatrix}, \quad \hat{e}_{ij}^0 = \begin{pmatrix} 0 & 0 & 0 & e_{14}^0 & 0 & e_{16}^0 \\ e_{21}^0 & e_{22}^0 & e_{23}^0 & 0 & e_{25}^0 & 0 \\ 0 & 0 & 0 & e_{34}^0 & 0 & e_{36}^0 \end{pmatrix},$$
$$\hat{\chi}_{ii'}^{\varepsilon 0} = \begin{pmatrix} \chi_{11}^{\varepsilon 0} & 0 & \chi_{13}^{\varepsilon 0} \\ 0 & \chi_{22}^{\varepsilon 0} & 0 \\ \chi_{13}^{\varepsilon 0} & 0 & \chi_{33}^{\varepsilon 0} \end{pmatrix}.$$

In the paraelectric phase all coefficients $e_{ij}^0 \equiv 0$.

Another terms in (1) describe the pseudospin part of hamiltonian. In particular, the second term in (1) is hamiltonian of short-range interactions:

$$\hat{H}_{\text{short}} = -2\sum_{qq'}\left(w_1\frac{\sigma_{q1}}{2}\frac{\sigma_{q2}}{2} + w_2\frac{\sigma_{q3}}{2}\frac{\sigma_{q4}}{2}\right)\left(\delta_{\mathbf{R}_q\mathbf{R}_{q'}} + \delta_{\mathbf{R}_q+\mathbf{R_c},\mathbf{R}_{q'}}\right).$$

In (2) σ_{qf} is the z-component of pseudospin operator, that describes the state of the f-th bond ($f = 1, 2, 3, 4$), in the q-th cell. The first Kronecker delta corresponds to the interaction between protons in the chains near the tetrahedra HPO_3 of type "I" (see Fig. 1), where the second one near the tetrahedra HPO_3 of type "II", $\mathbf{R_c}$ is the lattice vector along OZ-axis. Contributions into the energy of interactions between protons near tetrahedra of different type, as well as the mean values of the pseudospins $\eta_f = \langle\sigma_{qf}\rangle$, which are related to tetrahedra of different type, are identical.

Parameters w_1, w_2, which describe the short-range interactions within chains, are expanded linearly into series over strains ε_j:

$$w_1 = w^0 + \sum_l \delta_l\varepsilon_l + \delta_4\varepsilon_4 + \delta_6\varepsilon_6, \quad (l = 1, 2, 3, 5) \tag{2}$$

$$w_2 = w^0 + \sum_l \delta_l\varepsilon_l - \delta_4\varepsilon_4 - \delta_6\varepsilon_6.$$

The third term in (1) describes the long-range dipole-dipole interactions and indirect (through the lattice vibrations) interactions between protons, which are taken into account in mean field approximation:

$$\hat{H}_{\text{long}} = \frac{1}{2}\sum_{\substack{qq'\\ff'}} J_{ff'}(qq')\frac{\langle\sigma_{qf}\rangle}{2}\frac{\langle\sigma_{q'f'}\rangle}{2} - \sum_{\substack{qq'\\ff'}} J_{ff'}(qq')\frac{\langle\sigma_{q'f'}\rangle}{2}\frac{\sigma_{qf}}{2}. \tag{3}$$

Fourier transforms of interaction constants $J_{ff'} = \sum_{q'} J_{ff'}(qq')$ at $\mathbf{k} = 0$ are linearly expanded over the strains ε_j:

$$J_{\substack{11\\33}} = J_{11}^0 + \sum_l \psi_{11l}\varepsilon_l \pm \psi_{114}\varepsilon_4 \pm \psi_{116}\varepsilon_6, \quad J_{13} = J_{13}^0 + \sum_l \psi_{13l}\varepsilon_l + \psi_{134}\varepsilon_4 + \psi_{136}\varepsilon_6,$$

$$J_{\substack{12\\34}} = J_{12}^0 + \sum_l \psi_{12l}\varepsilon_l \pm \psi_{124}\varepsilon_4 \pm \psi_{126}\varepsilon_6, \quad J_{\substack{14\\23}} = J_{14}^0 + \sum_l \psi_{14l}\varepsilon_l \pm \psi_{144}\varepsilon_4 \pm \psi_{146}\varepsilon_6,$$

$$J_{\substack{22\\44}} = J_{22}^0 + \sum_l \psi_{22l}\varepsilon_l \pm \psi_{224}\varepsilon_4 \pm \psi_{226}\varepsilon_6, \quad J_{24} = J_{24}^0 + \sum_l \psi_{24l}\varepsilon_l + \psi_{244}\varepsilon_4 + \psi_{246}\varepsilon_6.$$

In result, (3) can be written as:

$$\hat{H}_{\text{long}} = NH^0 - \sum_q\sum_{f=1}^4 \mathcal{H}_f\frac{\sigma_{qf}}{2}, \tag{4}$$

where

$$H^0 = \sum_{f,f'=1}^4 \frac{1}{8}J_{ff'}\eta_f\eta_{f'}, \quad \mathcal{H}_f = \sum_{f'=1}^4 \frac{1}{2}J_{ff'}\eta_{f'}. \tag{5}$$

The fourth term in (1) describes interactions of pseudospins with external electric field:

$$\hat{H}_E = -\sum_{qf}\boldsymbol{\mu}_f\boldsymbol{E}\frac{\sigma_{qf}}{2}. \tag{6}$$

Here $\boldsymbol{\mu}_1 = (\mu_{13}^x, \mu_{13}^y, \mu_{13}^z)$, $\boldsymbol{\mu}_3 = (-\mu_{13}^x, \mu_{13}^y, -\mu_{13}^z)$, $\boldsymbol{\mu}_2 = (-\mu_{24}^x, -\mu_{24}^y, \mu_{24}^z)$, $\boldsymbol{\mu}_4 = (\mu_{24}^x, -\mu_{24}^y, -\mu_{24}^z)$ are the effective dipole moments per one pseudospin.

3. Piezoelectric characteristics of GPI

Two-particle cluster approximation is used for calculation of thermodynamic characteristics of GPI. In this approximation thermodynamic potential per one primitive cell is given by [7]:

$$g = \frac{G}{N} = U_{\text{seed}} + H^0 - 2\Big(w^0 + \sum_l \delta_l \varepsilon_l\Big) + 2k_{\text{B}}T \ln 2 - N\upsilon \sum_{j=1}^{6} \sigma_j \varepsilon_j$$

$$- \frac{1}{2}k_{\text{B}}T \sum_{f=1}^{4} \ln\big(1 - \eta_f^2\big) - 2k_{\text{B}}T \ln D. \tag{7}$$

where $\beta = \frac{1}{k_{\text{B}}T}$, k_{B} is the Boltzmann constant. Here, such notations are used:

$$D = \cosh n_1 + \cosh n_2 + a^2 \cosh n_3 + a^2 \cosh n_4$$

$$+ a a_{46} \cosh n_5 + \frac{a}{a_{46}} \cosh n_6 + a\, a_{46} \cosh n_7 + \frac{a}{a_{46}} \cosh n_8,$$

$$n_1 = \frac{1}{2}(y_1 + y_2 + y_3 + y_4), \quad n_2 = \frac{1}{2}(y_1 + y_2 - y_3 - y_4), \quad n_3 = \frac{1}{2}(y_1 - y_2 + y_3 - y_4),$$

$$n_4 = \frac{1}{2}(y_1 - y_2 - y_3 + y_4), \quad n_5 = \frac{1}{2}(y_1 - y_2 + y_3 + y_4), \quad n_6 = \frac{1}{2}(y_1 + y_2 + y_3 - y_4),$$

$$n_7 = \frac{1}{2}(-y_1 + y_2 + y_3 + y_4), \quad n_8 = \frac{1}{2}(y_1 + y_2 - y_3 + y_4).$$

$$y_f = \frac{1}{2}\ln\frac{1 + \eta_f}{1 - \eta_f} + \frac{\beta}{2}\sum_{f'=1}^{4}\frac{1}{2}J_{ff'}\eta_{f'} + \frac{\beta}{2}\boldsymbol{\mu}_f\boldsymbol{E}, \quad a = e^{-\beta(w^0 + \sum_l \delta_i \varepsilon_i)}, \quad a_{46} = e^{-\beta(\delta_4\varepsilon_4 + \delta_6\varepsilon_6)}.$$

Minimizing the thermodynamic potential the system of equations for the strains ε_j and the order parameters η_f, are obtained. Differentiating the thermodynamic potential over the fields E_1 and E_3 we obtain the expressions for polarizations P_1 and P_3 [7]:

$$P_1 = e_{14}^0 \varepsilon_4 + e_{16}^0 \varepsilon_6 + \chi_{11}^{\varepsilon 0} E_1 + \frac{1}{2\upsilon}[\mu_{13}^x(\eta_1 - \eta_3) - \mu_{24}^x(\eta_2 - \eta_4)], \tag{8}$$

$$P_3 = e_{34}^0 \varepsilon_4 + e_{66}^0 \varepsilon_6 + \chi_{33}^{\varepsilon 0} E_3 + \frac{1}{2\upsilon}[\mu_{13}^z(\eta_1 - \eta_3) + \mu_{24}^z(\eta_2 - \eta_4)].$$

Differentiating expressions (8) over strains ε_{1j} the expressions for isothermic coefficients of piezoelectric stress e_{1j}, e_{3j} of GPI are obtained:

$$e_{1j} = \left(\frac{\partial P_1}{\partial \varepsilon_l}\right)_{E_1} = e_{2j}^0 + \frac{1}{2\upsilon}[\mu_{13}^x(\dot{\eta}_{1\varepsilon_j} - \dot{\eta}_{3\varepsilon_j}) - \mu_{24}^x(\dot{\eta}_{2\varepsilon_j} - \dot{\eta}_{4\varepsilon_j})], \quad (j = 4, 6), \tag{9}$$

$$e_{3j} = \left(\frac{\partial P_3}{\partial \varepsilon_j}\right)_{E_3} = e_{3j}^0 + \frac{1}{2\upsilon}[\mu_{13}^z(\dot{\eta}_{1\varepsilon_j} - \dot{\eta}_{3\varepsilon_j}) + \mu_{24}^z(\dot{\eta}_{2\varepsilon_j} - \dot{\eta}_{4\varepsilon_j}), \quad (j = 4, 6). \tag{10}$$

where $\dot{\eta}_{1\varepsilon_l}$, $\dot{\eta}_{2\varepsilon_l}$, $\dot{\eta}_{3\varepsilon_l}$, $\dot{\eta}_{4\varepsilon_l}$ are the solutions of the following system of equations:

$$\begin{pmatrix} 2D - \varkappa_{11} & -\varkappa_{12} & -\varkappa_{13} & -\varkappa_{14} \\ -\varkappa_{21} & 2D - \varkappa_{22} & -\varkappa_{23} & -\varkappa_{24} \\ -\varkappa_{31} & -\varkappa_{32} & 2D - \varkappa_{33} & -\varkappa_{34} \\ -\varkappa_{41} & -\varkappa_{42} & -\varkappa_{43} & 2D - \varkappa_{44} \end{pmatrix} \times \begin{pmatrix} \dot{\eta}_{1\varepsilon_l} \\ \dot{\eta}_{2\varepsilon_l} \\ \dot{\eta}_{3\varepsilon_l} \\ \dot{\eta}_{4\varepsilon_l} \end{pmatrix} = \begin{pmatrix} \varkappa_1^{e_l} \\ \varkappa_2^{e_l} \\ \varkappa_3^{e_l} \\ \varkappa_4^{e_l} \end{pmatrix}.$$

Here the notations are used:

$$\varkappa_{f1} = \varkappa_{f11}(\varphi_1^+ + \beta\bar{\nu}_1^+) + \varkappa_{f12}(\beta\nu_2^+ + \beta\bar{\nu}_2^+) + \varkappa_{f13}(\varphi_1^- + \beta\bar{\nu}_1^-) + \varkappa_{f14}\beta(\nu_2^- + \beta\bar{\nu}_2^-),$$
$$\varkappa_{f2} = \varkappa_{f12}(\varphi_2^+ + \beta\bar{\nu}_3^+) + \varkappa_{f11}(\beta\nu_2^+ + \beta\bar{\nu}_2^+) + \varkappa_{f14}(\varphi_2^- + \beta\bar{\nu}_3^-) + \varkappa_{f13}(\beta\nu_2^- + \beta\bar{\nu}_2^+),$$
$$\varkappa_{f3} = \varkappa_{f11}(\varphi_3^+ - \beta\bar{\nu}_1^-) + \varkappa_{f12}(\beta\nu_2^+ - \beta\bar{\nu}_2^+) - \varkappa_{f13}(\varphi_3^- - \beta\bar{\nu}_1^+) - \varkappa_{f14}(\beta\nu_2^- - \beta\bar{\nu}_2^-),$$
$$\varkappa_{f4} = \varkappa_{f12}(\varphi_4^+ - \beta\bar{\nu}_3^-) + \varkappa_{f11}(\beta\nu_2^+ - \beta\bar{\nu}_2^-) - \varkappa_{f14}(\varphi_4^- - \beta\bar{\nu}_3^+) - \varkappa_{f13}(\beta\nu_2^- - \beta\bar{\nu}_2^+),$$

$$\varphi_{1,3}^\pm = \frac{1}{1-\eta_{1,3}^2} + \beta\nu_1^\pm, \qquad\qquad \varphi_{2,4}^\pm = \frac{1}{1-\eta_{2,4}^2} + \beta\nu_3^\pm,$$

$$\nu_l^\pm = \nu_l^{0\pm} + \left(\sum_{i=1}^3 \psi_{li}^\pm \varepsilon_i + \psi_{l5}^\pm \varepsilon_5\right), \qquad \bar{\nu}_l^\pm = \psi_{l4}^\pm \varepsilon_4 + \psi_{l6}^\pm \varepsilon_6,$$

$$\nu_1^{0\pm} = \frac{1}{4}(J_{11}^0 \pm J_{13}^0), \qquad\qquad \nu_2^{0\pm} = \frac{1}{4}(J_{12}^0 \pm J_{14}^0), \qquad \nu_3^{0\pm} = \frac{1}{4}(J_{22}^0 \pm J_{24}^0),$$

$$\psi_{1i}^\pm = \frac{1}{4}(\psi_{11i} \pm \psi_{13i}), \qquad\qquad \psi_{2i}^\pm = \frac{1}{4}(\psi_{12i} \pm \psi_{14i}), \qquad \psi_{3i}^\pm = \frac{1}{4}(\psi_{22i} \pm \psi_{24i}),$$

$$\varkappa_{\frac{1}{3}11} = (l_{1+3}^c + l_{5+6}^c) - \eta_{\frac{1}{3}}(l_{1+3}^s + l_{5+6}^s), \qquad \varkappa_{\frac{1}{3}12} = (l_{1-3}^c \mp l_{7-8}^c) - \eta_{\frac{1}{3}}(l_{1-3}^s + l_{7+8}^s),$$
$$\varkappa_{\frac{1}{3}13} = \pm(l_{2+4}^c + l_{7+8}^c) - \eta_{\frac{1}{3}}(l_{2+4}^s - l_{7-8}^s), \qquad \varkappa_{\frac{1}{3}14} = (\pm l_{2-4}^c - l_{5-6}^c) - \eta_{\frac{1}{3}}(l_{2-4}^s - l_{5-6}^s),$$
$$\varkappa_{\frac{2}{4}11} = (l_{1-3}^c \mp l_{5-6}^c) - \eta_{\frac{2}{4}}(l_{1+3}^s + l_{5+6}^s), \qquad \varkappa_{\frac{2}{4}12} = (l_{1+3}^c + l_{7+8}^c) - \eta_{\frac{2}{4}}(l_{1-3}^s + l_{7+8}^s),$$
$$\varkappa_{\frac{2}{4}13} = (\pm l_{2-4}^c - l_{7-8}^c) - \eta_{\frac{2}{4}}(l_{2+4}^s - l_{7-8}^s), \qquad \varkappa_{\frac{2}{4}14} = (\pm l_{2+4}^c \pm l_{5+6}^c) - \eta_{\frac{2}{4}}(l_{2-4}^s - l_{5-6}^s),$$
$$\varkappa_{\frac{1}{3}15} = (\mp l_{2-4}^c + l_{5-6}^c) - \eta_{\frac{1}{3}}(-l_{2-4}^s + l_{5-6}^s), \qquad \varkappa_{\frac{2}{4}15} = \mp(l_{2+4}^c + l_{5+6}^c) + \eta_{\frac{2}{4}}(-l_{2-4}^s + l_{5-6}^s),$$

$$l_{1\pm3}^c = \cosh n_1 \pm a^2 \cosh n_3; \qquad\qquad l_{2\pm4}^c = \cosh n_2 \pm a^2 \cosh n_4;$$
$$l_{1\pm3}^s = \sinh n_1 \pm a^2 \sinh n_3; \qquad\qquad l_{2\pm4}^s = \sinh n_2 \pm a^2 \sinh n_4;$$
$$l_{5\pm6}^c = a\,a_{46}\cosh n_5 \pm \frac{a}{a_{46}}\cosh n_6; \qquad l_{7\pm8}^c = a\,a_{46}\cosh n_7 \pm \frac{a}{a_{46}}\cosh n_8;$$
$$l_{5\pm6}^s = a\,a_{46}\sinh n_5 \pm \frac{a}{a_{46}}\sinh n_6; \qquad l_{7\pm8}^s = a\,a_{46}\sinh n_7 \pm \frac{a}{a_{46}}\sinh n_8,$$

$$\varkappa_f^{e_l} = \beta(\psi_{1l}^+ \varkappa_{f11} + \psi_{2l}^+ \varkappa_{f12})(\eta_1 + \eta_3) + \beta(\psi_{2l}^+ \varkappa_{f11} + \psi_{3l}^+ \varkappa_{f12})(\eta_2 + \eta_4)$$
$$+ \beta(\psi_{1l}^- \varkappa_{f13} + \psi_{2l}^- \varkappa_{f14})(\eta_1 - \eta_3) + \beta(\psi_{2l}^- \varkappa_{f13} + \psi_{3l}^- \varkappa_{f14})(\eta_2 - \eta_4) + 2\beta\delta_l(\rho_{f1} + \rho_{f2}),$$

$$\rho_{\frac{1}{3}2} = -l_{5+6}^s \pm l_{7-8}^s + \eta_{\frac{1}{3}}(l_{5+6}^c + l_{7+8}^c), \qquad \rho_{\frac{2}{4}1} = 2(l_{3\pm4}^s + \eta_{\frac{1}{3}}l_{3+4}^c),$$
$$\rho_{\frac{2}{4}2} = \pm l_{5-6}^s - l_{7+8}^s + \eta_{\frac{1}{3}}(l_{5+6}^c + l_{7+8}^c), \qquad \rho_{\frac{1}{3}j} = l_{5+6}^s \pm l_{7-8}^s + \eta_{\frac{1}{3}}(l_{5+6}^c - l_{7+8}^c),$$
$$\rho_{\frac{2}{4}j} = \mp l_{5-6}^s + l_{7+8}^s + \eta_{\frac{2}{4}}(l_{5+6}^c - l_{7+8}^c), \qquad l_{3\pm4}^s = a^2 \text{sh} n_3 \pm a^2 \text{sh} n_4, \quad l_{3+4}^c = a^2 \text{ch} n_3 + a^2 \text{ch} n_4.$$

Constants of piezoelectric stress are obtained by differentiation of electric field over strains at constant polarization, and they can be reduced to such form:

$$h_{1j} = \frac{e_{1j}}{\chi_{11}^\varepsilon}, \quad h_{3j} = \frac{e_{3j}}{\chi_{33}^\varepsilon}. \tag{11}$$

where the expressions for transverse dielectric permittivities χ_{11}^ε and χ_{33}^ε is given by [7]:

$$\chi_{11}^\varepsilon = \chi_{11}^{\varepsilon 0} + \frac{1}{2\upsilon\Delta}[\mu_{13}^x(\Delta_1^{\chi a} - \Delta_3^{\chi x}) - \mu_{24}^x(\Delta_2^{\chi x} - \Delta_4^{\chi x})], \tag{12}$$

$$\chi_{33}^\varepsilon = \chi_{33}^{\varepsilon 0} + \frac{1}{2\upsilon\Delta}[\mu_{13}^z(\Delta_1^{\chi z} - \Delta_3^{\chi z}) + \mu_{24}^c(\Delta_2^{\chi z} - \Delta_4^{\chi z})]. \tag{13}$$

Here such notation are used:

$$\Delta = \begin{vmatrix} 2D-\varkappa_{11} & -\varkappa_{12} & -\varkappa_{13} & -\varkappa_{14} \\ -\varkappa_{21} & 2D-\varkappa_{22} & -\varkappa_{23} & -\varkappa_{24} \\ -\varkappa_{31} & -\varkappa_{32} & 2D-\varkappa_{33} & -\varkappa_{34} \\ -\varkappa_{41} & -\varkappa_{42} & -\varkappa_{43} & 2D-\varkappa_{44} \end{vmatrix},$$

$$\Delta_1^{\chi\alpha} = \begin{vmatrix} \varkappa_1^{\chi\alpha} & -\varkappa_{12} & -\varkappa_{13} & -\varkappa_{14} \\ \varkappa_2^{\chi\alpha} & 2D-\varkappa_{22} & -\varkappa_{23} & -\varkappa_{24} \\ \varkappa_3^{\chi\alpha} & -\varkappa_{32} & 2D-\varkappa_{33} & -\varkappa_{34} \\ \varkappa_4^{\chi\alpha} & -\varkappa_{42} & -\varkappa_{43} & 2D-\varkappa_{44} \end{vmatrix}, \quad \Delta_3^{\chi\alpha} = \begin{vmatrix} 2D-\varkappa_{11} & -\varkappa_{12} & \varkappa_1^{\chi\alpha} & -\varkappa_{14} \\ -\varkappa_{21} & 2D-\varkappa_{22} & \varkappa_2^{\chi\alpha} & -\varkappa_{24} \\ -\varkappa_{31} & -\varkappa_{32} & \varkappa_3^{\chi\alpha} & -\varkappa_4 \\ -\varkappa_{41} & -\varkappa_{42} & \varkappa_4^{\chi\alpha} & 2D-\varkappa_{44} \end{vmatrix},$$

$$\Delta_2^{\chi\alpha} = \begin{vmatrix} 2D-\varkappa_{11} & \varkappa_1^{\chi\alpha} & -\varkappa_{13} & -\varkappa_{14} \\ -\varkappa_{21} & \varkappa_2^{\chi\alpha} & -\varkappa_{23} & -\varkappa_{24} \\ -\varkappa_{31} & \varkappa_3^{\chi\alpha} & 2D-\varkappa_{33} & -\varkappa_{34} \\ -\varkappa_{41} & \varkappa_4^{\chi\alpha} & -\varkappa_{43} & 2D-\varkappa_{44} \end{vmatrix}, \quad \Delta_4^{\chi\alpha} = \begin{vmatrix} 2D-\varkappa_{11} & -\varkappa_{12} & -\varkappa_{13} & \varkappa_1^{\chi\alpha} \\ -\varkappa_{21} & 2D-\varkappa_{22} & -\varkappa_{23} & \varkappa_2^{\chi\alpha} \\ -\varkappa_{31} & -\varkappa_{32} & 2D-\varkappa_{33} & \varkappa_2^{\chi\alpha} \\ -\varkappa_{41} & -\varkappa_{42} & -\varkappa_{43} & \varkappa_4^{\chi\alpha} \end{vmatrix},$$

where

$$\varkappa_f^{\chi x} = \varkappa_{f13}\beta\mu_{13}^x + \varkappa_{f15}\beta\mu_{24}^x, \quad \varkappa_f^{\chi y} = \varkappa_{f11}\beta\mu_{13}^y + \varkappa_{f12}\beta\mu_{24}^y, \quad \varkappa_f^{\chi z} = \varkappa_{f13}\beta\mu_{13}^z + \varkappa_{f14}\beta\mu_{24}^z.$$

4. The results of numerical calculations

For numerical calculation of dielectric and piezoelectric characteristics of GPI we use the parameters determined in [7] from the condition of agreement of calculated characteristics with experimental data, which are enumerated below.

— The parameter of the short-range interactions $w_0/k_B = 800\,\text{K}$;
— The parameters of the long-range interactions
  $\tilde{\nu}_1^{0+} = \tilde{\nu}_2^{0+} = \tilde{\nu}_3^{0+} = 3.065\,\text{K}$, $\tilde{\nu}_1^{0-} = \tilde{\nu}_2^{0-} = \tilde{\nu}_3^{0-} = 0.05\,\text{K}$, where $\tilde{\nu}_f^{0\pm} = \nu_f^{0\pm}/k_B$.
— The optimal values of the strain potentials:
  $\tilde{\delta}_1 = 500\,\text{K}$, $\tilde{\delta}_2 = 600\,\text{K}$, $\tilde{\delta}_3 = 500\,\text{K}$, $\tilde{\delta}_4 = 150\,\text{K}$, $\tilde{\delta}_5 = 100\,\text{K}$, $\tilde{\delta}_6 = 150\,\text{K}$; $\tilde{\delta}_i = \delta_i/k_B$;
  $\tilde{\psi}_{f1}^+ = 93.6\,\text{K}$, $\tilde{\psi}_{f2}^+ = 252.5\,\text{K}$, $\tilde{\psi}_{f3}^+ = 110.7\,\text{K}$, $\tilde{\psi}_{f4}^+ = \tilde{\psi}_{f6}^+ = \tilde{\psi}_{f4}^- = \tilde{\psi}_{f6}^- = 79.5\,\text{K}$, $\tilde{\psi}_{f5}^+ = 22.7\,\text{K}$,
  $\tilde{\psi}_{f1}^- = \tilde{\psi}_{f2}^- = \tilde{\psi}_{f3}^- = \tilde{\psi}_{f5}^- = 0\,\text{K}$, where $\tilde{\psi}_{fi}^\pm = \psi_{fi}^\pm/k_B$.
— The components of effective dipole moments in paraelectric phase are equal to
  $\mu_{13}^x = 0.4 \cdot 10^{-18}\text{esu·cm}$; $\mu_{13}^y = 4.05 \cdot 10^{-18}\text{esu·cm}$; $\mu_{13}^z = 4.2 \cdot 10^{-18}\text{esu·cm}$;
  $\mu_{24}^x = 2.3 \cdot 10^{-18}\text{esu·cm}$; $\mu_{24}^y = 3.0 \cdot 10^{-18}\text{esu·cm}$; $\mu_{24}^z = 2.2 \cdot 10^{-18}\text{esu·cm}$.
  In the ferroelectric phase the y-component of the first dipole moment is $\mu_{13\text{ferro}}^y = 3.82 \cdot 10^{-18}\text{esu·cm}$, and other components are such as in the paraelectric phase.
— The volume of primitive cell of GPI: $v = 0.601 \cdot 10^{-21}\,\text{cm}^3$.
— The "seed" coefficients of piezoelectric stress e_{ij}^0, "seed" dielectric susceptibilities $\chi_{ij}^{\varepsilon 0}$ and "seed" elastic constants c_{ij}^{E0} are obtained as follow:
  $e_{ij}^0 = 0.0\frac{\text{esu}}{\text{cm}^2}$; $\chi_{11}^{\varepsilon 0} = 0.1$, $\chi_{22}^{\varepsilon 0} = 0.403$, $\chi_{33}^{\varepsilon 0} = 0.5$, $\chi_{31}^{\varepsilon 0} = 0.0$; $c_{11}^{0E} = 269.1\,\text{kbar}$, $c_{12}^{E0} = 145\,\text{kbar}$,
  $c_{13}^{E0} = 116.4\,\text{kbar}$, $c_{15}^{E0} = 39.1\,\text{kbar}$, $c_{22}^{E0} = (649.9 - 0.4(T-T_c))\,\text{kbar}$,
  $c_{23}^{E0} = 203.8\,\text{kbar}$, $c_{25}^{E0} = 56.4\,\text{kbar}$, $c_{33}^{E0} = 244.1\,\text{kbar}$, $c_{35}^{E0} = -28.4\,\text{kbar}$,
  $c_{55}^{E0} = 85.4\,\text{kbar}$, $c_{44}^{E0} = 153.1\,\text{kbar}$, $c_{46}^{E0} = -11\,\text{kbar}$, $c_{66}^{E0} = 118.8\,\text{kbar}$.

Now let us dwell on the obtained results. The temperature dependences of the coefficients of piezoelectric stress e_{1j}, e_{3j} and constants of piezoelectric stress h_{1j}, h_{3j} are presented in Fig. 2. These coefficients are equal to zero in the paraelectric phase, because there exists an inversion center. In the ferroelectric phase the coefficients e_{1j} and e_{3j}, unlike e_{2l}, do not go to infinity at $T \to T_c$; they together with the coefficients h_{1j}, h_{3j} slightly change and go to zero at the T_c point.
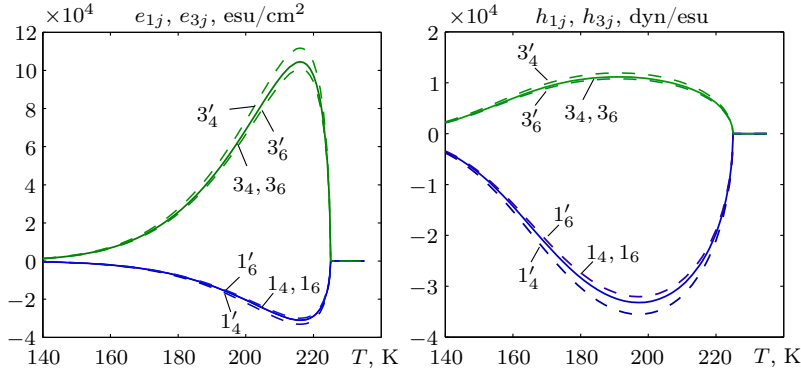
At the low temperatures they also go to zero, because the order parameters $\eta_f \to 1$ and weakly react on the lattice strains. As one can see from (9) and (10), the contributions to the coefficients e_{1j} from the pseudospins 1 and 2 partially compensate each other, whereas in the case of e_{3j} they supplement each other. Consequently, the coefficients e_{3j} have larger values than e_{1j}. Besides, the coefficients e_{1j} are negative, because the effective dipole moment of the second pseudospin μ_{24}^x is larger than μ_{13}^x. However,

Fig. 2. The temperature dependences of the piezoelectric coefficients e_{1j} (curves 1_j, $1'_j$), e_{3j} (3_j, $3'_j$), h_{1j} (1_j, $1'_j$) and h_{3j} (3_j, $3'_j$) of GPI crystal. The curves 1_j, 3_j are calculated at $\tilde\psi_{f4}^+ = \tilde\psi_{f6}^+ = 140$ K and the curves $1'_j$, $3'_j$ — at $\tilde\psi_{f4}^+ = 150$ K, $\tilde\psi_{f6}^+ = 130$ K.

the coefficients h_{3j} have smaller values than h_{1j}, because the transverse dielectric permittivity χ_{33}^ε, which is contained in (11), is of one order of magnitude larger than χ_{11}^ε (see [7]). The values of the coefficients of piezoelectric stress e_{1j} and constants of piezoelectric stress h_{1j} depend on the parameters $\tilde\psi_{f4}^+$, and the values of e_{3j} and h_{3j} depend on the parameters $\tilde\psi_{f6}^+$. If these parameters are equal, than $e_{14} = e_{16}$, $e_{34} = e_{36}$, $h_{14} = h_{16}$, $h_{34} = h_{36}$. In the case of different values of $\tilde\psi_{f4}^+$ and $\tilde\psi_{f6}^+$, the values of respective piezoelectric coefficients are different (dashed lines in Fig. 2). The final set of parameters $\tilde\psi_{f4}^+$ and $\tilde\psi_{f6}^+$ will be possible after carrying out of experimental measurements of the temperature dependences of e_{1j}, e_{3j} and h_{1j}, h_{3j}.
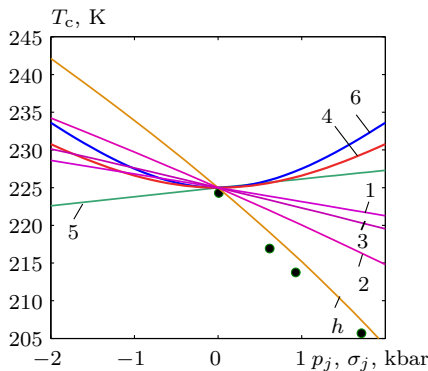

Now let us consider the influence of mechanical stresses on the piezoelectric coefficients. The hydrostatic pressure p_i, uniaxial pressures p_1, p_2, p_3 and shear stress σ_5 do not change the symmetry of GPI crystal. As was determined in [7], application of these pressures leads to weakening of the interactions between pseudospins, in consequence of this the phase transition temperature T_c linearly decreases with pressure (see Fig. 3, curves h, 1, 2, 3). The shear stress σ_5, on the contrary, strengthens interactions and increases the temperature T_c (see Fig. 3, curve 5), This leads to shift of the curves $e_{1j}(T)$, $e_{3j}(T)$, $h_{1j}(T)$ and $h_{3j}(T)$ to the lower temperatures under pressures and to the higher temperatures under stress σ_5 (see Fig. 4, curves h, 1, 2, 3, 5). Besides, at the constant deviation of temperature from the phase transition point $\Delta T = T - T_] = -3$ K the piezoelectric coefficients $e_{1j}(T)$, $e_{3j}(T)$, $h_{1j}(T)$, $h_{3j}(T)$ linearly increase with pressures and linearly decrease with stress σ_5 (see Fig. 5, curves h, 1, 2, 3, 5). It is caused by faster weakening

Fig. 3. Dependences of the phase transition temperature T_c of GPI crystal on hydrostatic pressure (curve h), uniaxial pressures p_1 (1), p_2 (2), p_3 (3) and shear stresses σ_4 (4), σ_5 (5), σ_6 (6) [7]. Symbols '•' are experimental data [8].

of long-range interactions in comparison with short-range interactions under pressures and by faster strengthening of long-range interactions in comparison with short-range interactions under shear stress σ_5. It should be noted that among the considered above pressures and stress the strongest effect is the effect of hydrostatic pressure p_h, and the weakest one is the effect of shear stress σ_5.

In [7] it was determined that the shear stresses σ_4, σ_6 decrease the symmetry of crystal. As a result, the components of spontaneous polarization P_1 and P_3 appears in the plane XZ (see Fig. 6); and the dependence $T_c(\sigma_{4,6})$ is nearly hyperbolic cosine (see Fig. 3, curves 4, 6). Under nonzero stresses σ_4, σ_6 small changes in strains $d\varepsilon_4$, $d\varepsilon_6$ are accompanied by change in temperature dT_c and by shift of
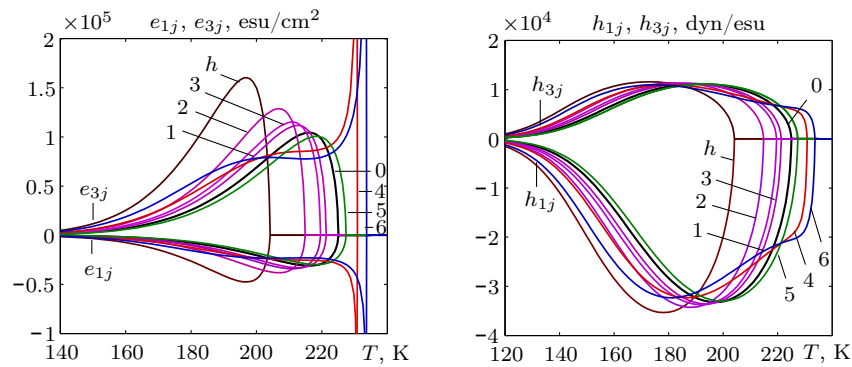
Fig. 4. The temperature dependences of the piezoelectric coefficients e_{1j}, e_{3j}, h_{1j} and h_{3j} of GPI crystal at the absence of any pressures and stresses (curve 0), under hydrostatic pressure (curve h), uniaxial pressures p_1 (1), p_2 (2), p_3 (3) and shear stresses σ_4 (4), σ_5 (5), σ_6 (6). The value of the pressures is equal to 2 kbar.
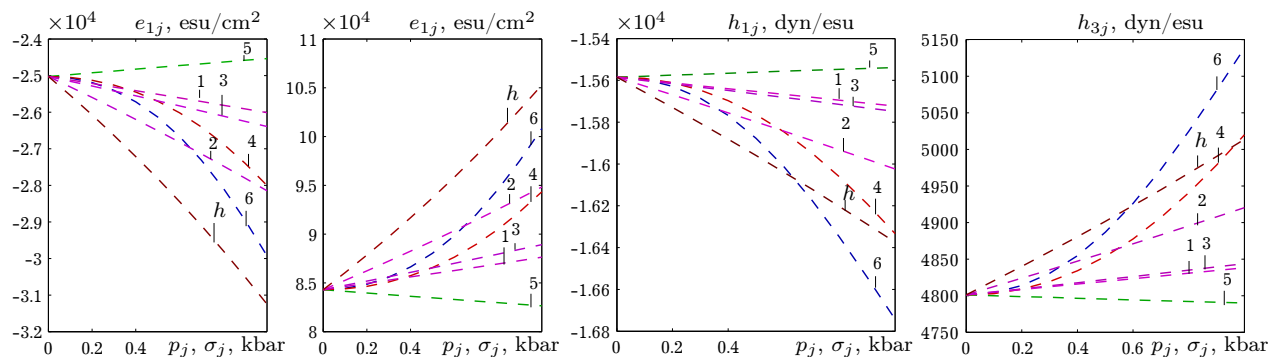
Fig. 5. Dependences of the piezoelectric coefficients e_{1j}, e_{3j}, h_{1j} and h_{3j} of GPI crystal on hydrostatic pressure (curve h), uniaxial pressures p_1 (1), p_2 (2), p_3 (3) and shear stresses σ_4 (4), σ_5 (5), σ_6 (6) at the deviation of temperature $\Delta T = -3\,\mathrm{K}$.
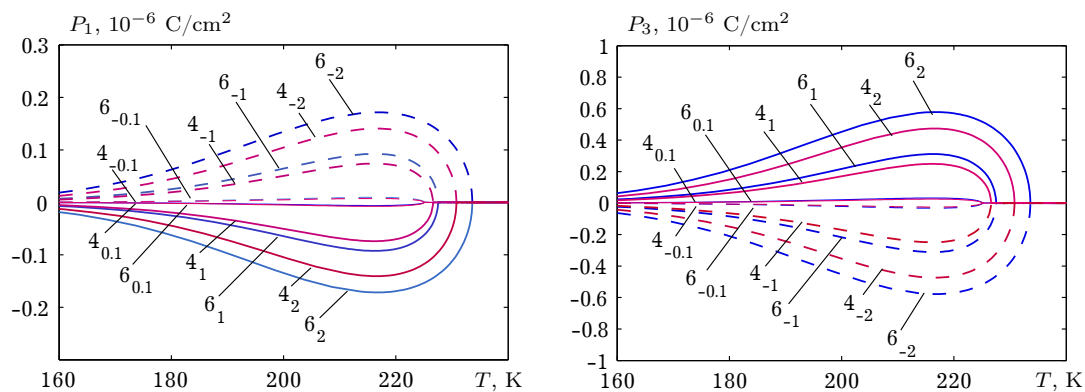

Fig. 6. The temperature dependences of polarizations P_1 and P_3 of GPI crystal at different stresses $\sigma_{4,6}$ [7]. Numbers of lines 4 and 6 mean the direction of applied stress σ_4 and σ_6 respectively, the inferior index shows value of the stresses (kbar).

the curves $P_1(T)$ and $P_3(T)$ to higher temperatures. Since $dP_i/dT \to \infty$ near the phase transition temperature, then $dP_i/d\varepsilon_4 \to \infty$, $dP_i/d\varepsilon_6 \to \infty$. As a result, the temperature dependences $e_{1j}(T)$, $e_{3j}(T)$ diverge in the T_c point (see Fig. 4, curves 4, 6), and the dependences $e_{1j}(T)$, $e_{3j}(T)$ on the stresses σ_4, σ_6 at constant $\Delta T = -3K$ are nonlinearly increasing in magnitude (see Fig. 5, curves 4, 6). The piezoelectric coefficients h_{1j}, h_{3j} are finite, because as was shown in [7], the transverse components of susceptibility χ_{11}^ε and χ_{33}^ε, which appear in (11), also diverge in the T_c point.

Now let us consider the influence of transverse electric fields E_1 and E_3 on the piezoelectric coefficients. As was shown in [6], these fields decrease the temperature T_c proportionally to E_1^2 and E_3^2, respectively. In Fig. 7 there are presented the temperature dependences of the piezoelectric coefficients
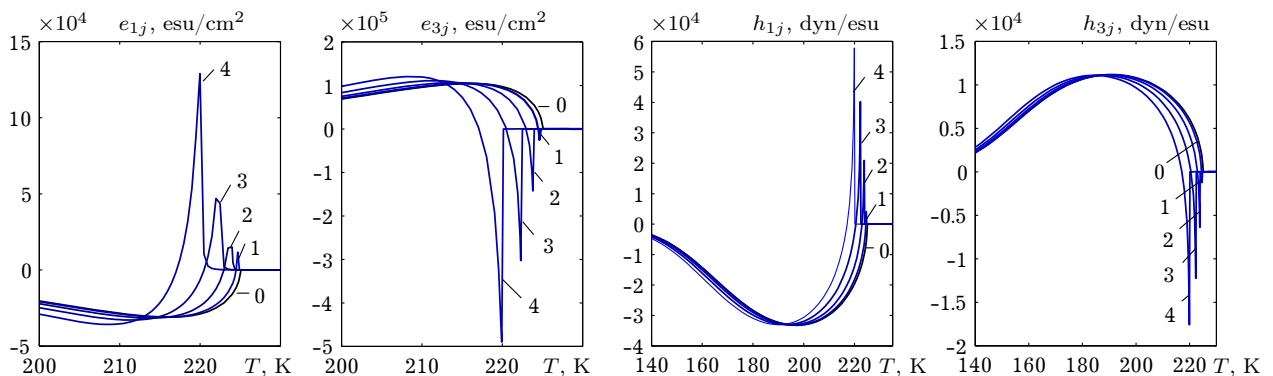

Fig. 7. The temperature dependences of the piezoelectric coefficients e_{1j}, e_{3j}, h_{1j} and h_{3j} of GPI crystal at different values of the electric field E_3 (MV/m): $0.0 - 0$; $1.0 - 1$; $2.0 - 2$; $3.0 - 3$; $4.0 - 4$.

e_{1j}, e_{3j}, h_{1j} and h_{3j} of GPI crystal at different values of the transverse electric field E_3. Under the influence of field E_3 in paraelectric phase the centre of inversion disappears, but reflection plane ac remains. Therefore the polarizations of both sublattices (the chains "A" and "B" in Fig. 1) are equal in direction and modulus. At small shear strain ε_4 or ε_6 the interactions between pseudospins in the chain "A" become stronger, but in the chain "B" they become weaker. The nascent changes in both sublattice polarizations mutually compensate each other, and the total polarization in the plane ac does not change. That is why the coefficients e_{1j}, e_{3j}, h_{1j} and h_{3j} are equal to zero.

In the ferroelectric phase the chains ""A" and "B" are ordered in the opposite directions. Therefore the weakening of interactions in the chain "B" in the presence of the stress ε_4 or ε_6 leads to the same sign of the changes in polarizations of sublattices. As a result, the piezoelectric coefficients are nonzero.

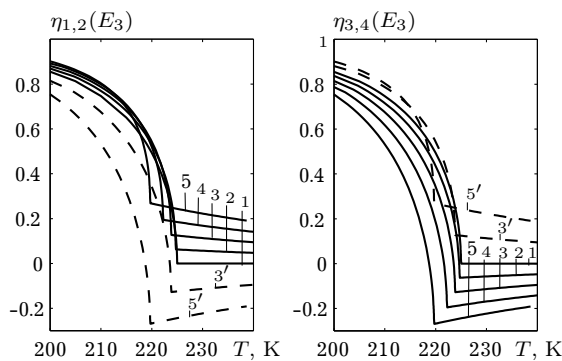**Fig. 8.** The temperature dependences of the order parameters η_f of the GPI crystal at different values of the electric field E_3(MV/m): $0.0 - 1$; $1.0 - 2$; $2.0 - 3$; $3.0 - 4$; $4.0 - 5$; $-2.0 - 3'$; $-4.0 - 5'$.

As was shown in [6], in the presence of electric field E_3 the order parameters η_3, η_4 decrease stronger than the order parameters η_1, η_2 increase (see Fig. 8). In result, the chain "B" becomes more sensitive to the strains and external fields in comparison with the chain "A" and in comparison with the case of zero field. At the low temperatures, when the order parameters are close to saturation, the strains ε_4 or ε_6 additionally weakening interactions in the chain "B". Then the expressions $\dot{\eta}_{3\varepsilon_l}$, $\dot{\eta}_{4\varepsilon_l}$, which appear in (10), are negative and larger in magnitude than at zero field. That is why the piezoelectric coefficients e_{1j}, e_{3j}, h_{1j} and h_{3j} increase in magnitude at the temperatures far from T_c ($T < 210$ K for e_{1j}, e_{3j} and $T < 180$ K for h_{1j}, h_{3j}, in Fig. 7) with increasing of electric field strength E_3.

At the temperatures close to T_c in the presence of field E_3 the protons in the chain "B" are almost fully disordered. In the presence of shear stresses the ordering in the chain "A" increases. Interchain interactions leads to increasing of antiparallel ordering in the chain "B". Consequently, the increment of polarization of the chain "B" appears, which is opposite in sign to the increment of polarization of the chain "A", and larger in magnitude. In result, the piezoelectric coefficients e_{1j}, e_{3j}, h_{1j} and h_{3j} decrease with strengthening of field, and there appears the negative peak near T_c ($T \lesssim T_c$ in Fig. 7), which is finite in magnitude.

In the presence of positive field E_1 and positive shear strains the equilibrium values of the order parameters reverse their signs. Consequently, the coefficients e_{1j}, e_{3j}, h_{1j} and h_{3j} in the presence of this field also reverse their signs (see Fig. 9). The effect of field E_1 is similar to the effect of field E_3, but of one order of magnitude larger.
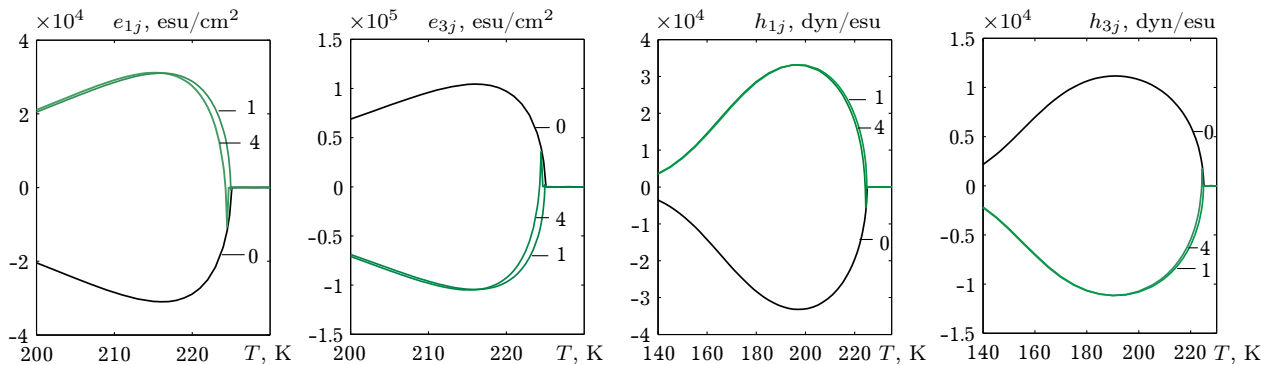

Fig. 9. The temperature dependences of the piezoelectric coefficients e_{1j}, e_{3j}, h_{1j} and h_{3j} of GPI crystal at different values of the electric field E_1 (MV/m): $0.0 - 0$; $1.0 - 1$; $4.0 - 4$.

Character of changes of the piezoelectric coefficients e_{1j}, e_{3j}, h_{1j} and h_{3j} with increasing of electric fields E_3 and E_1 at the deviations of temperature $\Delta T = -3$ K and -10 K is presented in Fig. 10.
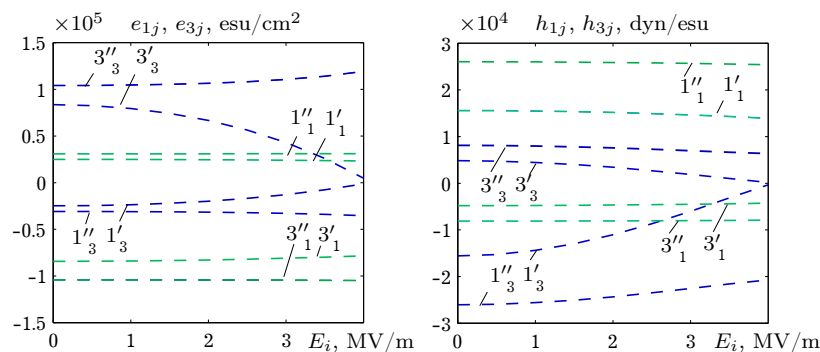

Fig. 10. Dependences of the piezoelectric coefficients e_{1j}, e_{3j}, h_{1j} i h_{3j} of GPI crystal on electric fields E_1 and E_3 at different temperatures. Number of line 1 or 3 means the coefficients e_{1j}, h_{1j} or e_{3j}, h_{3j}, respectively; inferior index 1 or 3 means the external field E_1 or E_3, respectively; prime or double prime means the temperature $\Delta T = -3$ K or -10 K, respectively.

5. Conclusions

The transverse piezoelectric coefficients e_{1j} and e_{3j}, in contrast to the longitudinal coefficients e_{2j}, are finite in the absence of external fields and mechanical stresses. The coefficients e_{3j}, h_{3j} are positive but e_{1j}, h_{1j} are negative. The hydrostatic p_h and uniaxial pressures p_1, p_2, p_3, and also shear stress σ_5 change the temperature T_c proportionally to the applied pressures, but qualitatively do not change their behaviour. The shear stresses σ_4, σ_6 leads to divergence of the coefficients e_{1j}, e_{3j} at the temperature T_c, but qualitatively do not change the coefficients h_{1j}, h_{3j}. The transverse electric fields E_1 and E_3 at the low temperatures, far from T_c, increase the piezoelectric coefficients in magnitude, but at the temperatures, close to T_c the finite negative peak appears. In the paraelectric phase they remain equal to zero even in the presence of mechanical stresses or transverse electric fields. Since there are not carried out any experimental measurements of the coefficients e_{1j}, e_{3j}, h_{1j} and h_{3j}, then obtained in this work their temperature, field and pressure dependences for GPI crystal have character of predictions.

[1] Dacko S., Czapla Z., Baran J., Drozd M. Ferroelectricity in Gly·H$_3$PO$_3$ crystal. Physics Letters A. **223** (3), 217–220 (1996).

[2] Stasyuk I., Czapla Z., Dacko S., Velychko O. Dielectric anomalies and phase transition in glycinium phosphite crystal under the influence of a transverse electric field. J. Phys.: Condens Matter. **16** (12), 1963 (2004).

[3] Zachek I. R., Shchur Ya, Levitskii R. R., Vdovych A. S. Thermodynamic properties of ferroelectric NH$_3$CH$_2$COOH·H$_2$PO$_3$ crystal. Physica B. **520**, 164–173 (2017).

[4] Zachek I. R., Levitskii R. R., Vdovych A. S. The effect of hydrostatic pressure on thermodynamic characteristics of NH$_3$CH$_2$COOH·H$_2$PO$_3$ type ferroelectric materials. Condens. Matter Phys. **20** (4), 43707 (2017).

[5] Zachek I. R., Levitskii R. R., Vdovych A. S. The influence of uniaxial pressures on thermodynamic properties of the GPI ferroelectric. J. Phys. Study. **21**, 1704 (2017), (in Ukrainian).

[6] Zachek I. R., Levitskii R. R., Vdovych A. S., Stasyuk I. V. Influence of electric fields on thermodynamic properties of GPI ferroelectric. Condens. Matter Phys. **20** (2), 23706 (2017).

[7] Zachek I. R., Levitskii R. R., Vdovych A. S. Deformation effects in glycinium phosphite ferroelectric. Condens. Matter Phys. **21** (3), 33702 (2018).

[8] Yasuda N., Sakurai T., Czapla Z. Effects of hydrostatic pressure on the paraelectric–ferroelectric phase transition in glycine phosphite (Gly·H$_3$PO$_3$). J. Phys.: Condens Matter. **9** (33), L347 (1997).

Розрахунок поперечних п'єзоелектричних характеристик квазіодновимірного сегнетоелектрика фосфіту гліцину

Вдович А.[1], Зачек І.[2], Левицький Р.[1]

[2]*Інститут фізики конденсованих систем НАН України,*
вул. Свєнціцького, 1, Львів, 79011, Україна
[1]*Національний університет "Львівська політехніка",*
вул. С. Бандери, 12, Львів, 79013, Україна

Для дослідження п'єзоелектричних характеристик кристала фосфіту гліцину використано модифіковану модель фосфіту гліцину з урахування п'єзоелектричного зв'язку структурних елементів, які впорядковуються, з деформаціями ґратки. В наближенні двочастинкового кластера розраховано поперечні п'єзоелектричні коефіцієнти. Досліджено вплив гідростатичного, одновісних тисків, зсувних напруг і поперечних електричних полів на поперечні п'єзоелектричні характеристики кристала.

Ключові слова: *сегнетоелектрики, фазовий перехід, п'єзоелектричні коефіцієнти, вплив тиску, вплив поля.*

2000 MSC: 82D45, 82B20

УДК: 536.96, 537.226536.96, 537.226(4, 82, 83, 86)